Separation Science and Technology
Publication details, including instructions for authors and subscription information:
http://www.informaworld.com/smpp/title~content=t713708471

Multigradient Dielectrophoresis: Wire Grid Matrix Optimization and Current Modelization at High Loading

Allen L. Shalom[ab]; Francis Lancelot[a]; Israel J. Lin[c]
[a] ELECTROCHEMISTRY DEPARTMENT, ECOLE DES MINES DE SAINT-ETIENNE, SAINT-ETIENNE CÉDEX, FRANCE [b] Benchmark, Structural Ceramics Corp., Buffalo, New York [c] MINERAL ENGINEERING DEPARTMENT, TECHNION ISRAEL INSTITUTE OF TECHNOLOGY, HAIFA, ISRAEL

To cite this Article Shalom, Allen L. , Lancelot, Francis and Lin, Israel J.(1989) 'Multigradient Dielectrophoresis: Wire Grid Matrix Optimization and Current Modelization at High Loading', Separation Science and Technology, 24: 3, 179 — 197
To link to this Article: DOI: 10.1080/01496398908049762
URL: http://dx.doi.org/10.1080/01496398908049762

SEPARATION SCIENCE AND TECHNOLOGY, 24(3&4), pp. 179-197, 1989

Multigradient Dielectrophoresis: Wire Grid Matrix Optimization and Current Modelization at High Loading

ALLEN L. SHALOM,*† and FRANCIS LANCELOT

ELECTROCHEMISTRY DEPARTMENT
ECOLE DES MINES DE SAINT-ETIENNE
158 COURS FAURIEL, 42023 SAINT-ETIENNE CÉDEX, FRANCE

ISRAEL J. LIN

MINERAL ENGINEERING DEPARTMENT
TECHNION
ISRAEL INSTITUTE OF TECHNOLOGY
HAIFA 32000, ISRAEL

Abstract

The various processes for separation with electric fields are briefly recalled with emphasis on dielectrophoresis. For dielectrophoretic filtration in nonaqueous liquids, a wire matrix optimization study shows that wires must be as thin as possible to maximize forces and at a distance to radius ratio below 5 for the best use of the electrified space. A model is proposed for the variation of the electric current measured as particle buildup is progressing. Numerical calculations are reported demonstrating the importance of transient effects. It is also mentioned that a more sophisticated approach incorporating the nonlinear behavior of conductivity vs field intensity is adequate to take into account effects occurring at high field intensities. Finally, practical design considerations are presented.

I. INTRODUCTION

The use of electric fields for processing particulates has been common from the beginning of the century in numerous areas of modern

*Present address: Benchmark, Structural Ceramics Corp., 2500 Walden Avenue, Buffalo, New York 14225.

†To whom correspondence should be addressed.

technology involving handling and separation of particles according to their electrical properties. Apart from the dry processes which are well known (*14*), those involving particles in liquids include printing, biophysical (*2*), petrochemical (*4*), electrochemical (*13*, *22*), as well as mineral processing applications (*9*). In the limited context of dielectrophoretic separation, which is governed by neutral particles migration in nonuniform dc or ac fields, a review of the diverse possibilities has been given by Lin and Benguigui (*11*).

The particles can be solid, liquid, or gaseous, while the fluid may be a liquid or a gas. Separation of the particles (S-S) or the particles and the fluid (S-L) is accomplished when the components have sufficiently different polarization characteristics. Thus, the process may consist in solid/solid (*9*), liquid/liquid (*23*), solid/liquid (*4*), gas/liquid (*8*), or solid/gas (*24*) separation and in biological applications may even differentiate between living and dead cells (*7*). Phase segregation can be performed in various ways. The different methods used can be classified in four main categories: dipole coalescence (*21*), deflection (*9*), trapping (*4*), and levitation (*12*). In these various techniques the desired split is obtained by judicious exploitation of geometric (particle size and shape), physical (permittivities, conductivities, densities), and operational (flow rate, field intensity and frequency, temperature) parameters. An interesting development initiated by the Petrolite Co. (*21*) and Gulf Co. (*4*) is covered by various patents. It consists of a separation cell made of two concentric electrodes between which glass beads are used to produce high field gradients responsible for trapping of the particulates. This technique compares favorably with the older dipole-coalescence method (*21*) which requires a relatively high dispersed phase concentration in order to be effective. In this context, research is being done on various matrices which would yield better results than glass beads. As a result of the experience accumulated in other areas of the separation technology—in particular magnetic separation—the main effort centers on fine rod matrices capable of producing high gradients. Clearly their main advantage is due to their very low packing densities which allow for efficient and easy cleaning.

In recent papers (*18*, *19*) an overview of the various theoretical aspects of matrix dielectrophoresis has been presented with emphasis on the main parameters governing the process. The matrix type is an important factor in separation efficiency, power consumption, pressure drop, feed/flush cycle length, etc. Hence it is of paramount importance to optimize the choice of a suitable matrix and to understand its behavior in an industrial environment. The principal matrix parameters are polarizability factor, element size and shape, and packing density.

Two main matrix types are to be considered in dealing with dielectric filtration: 1) a nonconductive one within a field applied by flat or concentric electrodes, and 2) a conductive one where the matrix is constituted of wire electrodes.

In the first approach a matrix (beads, rods) subjected to a uniform field (dc, ac, pulsed, uniform or not) distorts the field lines and generates high gradients in the vicinity of the elements. This technique is simple since it essentially involves a plate condenser filled, e.g., with beads (*11*). It has been used with success by Gulf and Petrolite (*4*, *10*) for petrochemical applications such as purification of fuel (removal of water drops and fine particulates down to colloidal size). Its main drawback is difficulty in scaling-up because it requires either very high voltages (necessitating costly and potentially hazardous power supplies) or recourse to multiple cells (concentric or in a linear array). Moreover, beads are not too satisfactory since they are hard to clean and occupy about 65% of the elctrified space.

In the second approach, rods or grids must be used. Here the matrix consists of parallel metal grids of alternate polarity (Fig. 1) which, given sufficiently close spacing and thin wires, yield a highly nonuniform applied field. This approach was first described and experimented with

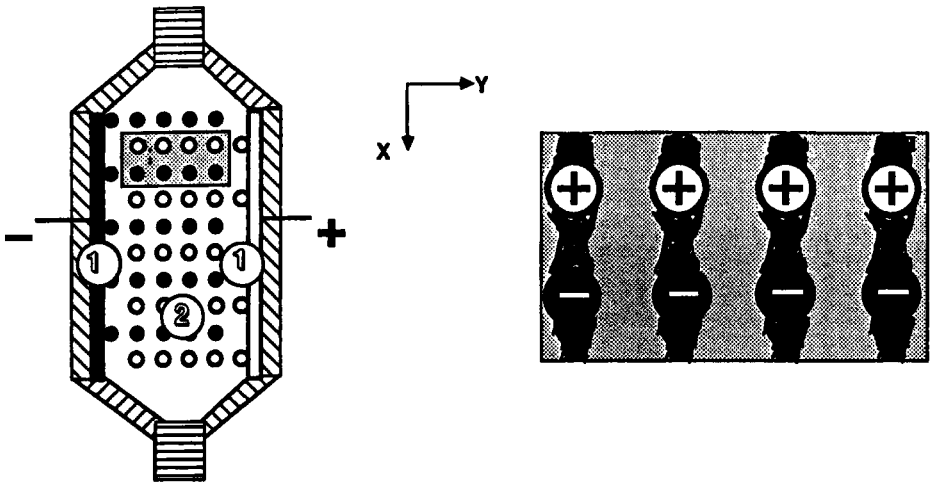

FIG. 1. Schematic representation of a grid filter: (1) flat electrodes; (2) wire grids connected alternately to positive (white) and negative (black) electrodes. The shaded area is shown in a closeup on the right to emphasize the particle buildup at saturation loading.

by Walkenhorst (*20*) for dust filtration from an air stream. For best results, wire size and spacing have to be optimized.

II. MATRIX OPTIMIZATION WITH TWO-WIRE MODEL

Figure 2 shows the field distribution for the two-wire case (*1*), which is fairly representative of the configuration obtained with grids of alternate polarity. In such a system, when the wire radius R is small compared to the spacing $2d$ of the wires, the latter may be regarded as lines of charge of negligible thickness without mutual influence. By contrast, when d/R is of the order of 1 to 10, the equivalent lines of charge are spaced at much less than $2d$; in these circumstances a high charge density is generated on the

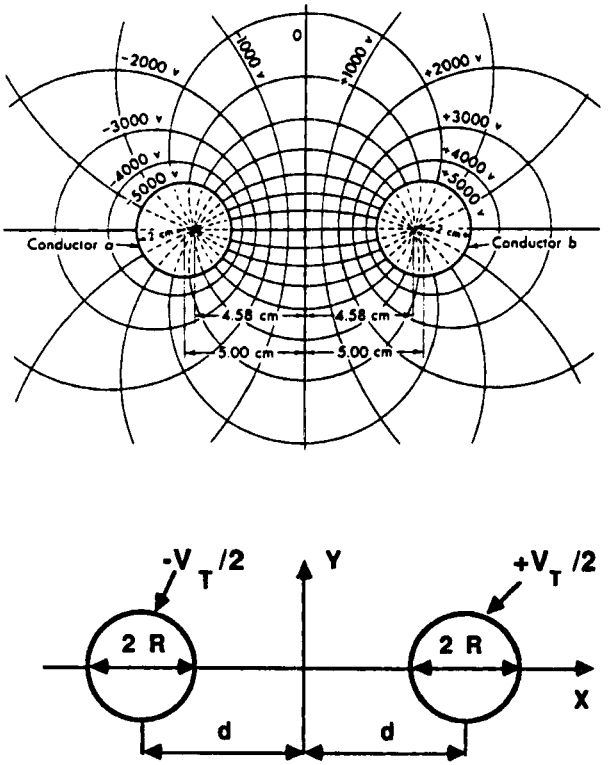

FIG. 2. Flow and potential lines for a pair of close wires (*1*).

wires as a result of Coulomb attraction between lines of opposite polarity. Thus, totally dissimilar behaviors prevail in the two cases.

A mathematical analysis is given below based on Ramo et al. (*17*) who put forward the following expression for the potential, ϕ:

$$\phi = \frac{V_T}{4 \cosh^{-1}\left(\frac{d}{R}\right)} \ln \frac{(X - C)^2 + Y^2}{(X + C)^2 + Y^2} \tag{1}$$

where $C = (d^2 - R^2)^{1/2}$ and V_T is the voltage applied to the wires. Since the field is stronger along the X-axis, a good notion of what can be expected is obtained by studying the pattern along this axis. Thus for $Y = 0$ we have

$$\phi_X = \frac{V_T}{2 \cosh^{-1}\left(\frac{d}{R}\right)} \ln \frac{X - C}{X + C} \tag{2}$$

yielding for the X-component of the field:

$$E_X = -\frac{d\phi_X}{dX} = -\frac{V_T C}{(X^2 - C^2) \cosh^{-1}\left(\frac{d}{R}\right)} \tag{3}$$

Clearly, the field is strongest at the surface of the wires and weakest halfway between them. Using Eq. (3):

$$E_{max} = \frac{V_T C}{2R(d - R) \cosh^{-1}\left(\frac{d}{R}\right)}, \quad \text{at } X = d - R \tag{4}$$

$$E_{min} = \frac{V_T}{C \cosh^{-1}\left(\frac{d}{R}\right)}, \quad \text{at } X = 0 \tag{5}$$

Best results for a given filter are expected at the breakdown voltage, V_b, which is the maximum voltage preceding a sudden increase of the electric current. Accordingly, all calculations should be carried out at this voltage, given as

$$V_b = \frac{V_T}{2(d-R)} = \text{constant} \tag{6}$$

The average X-gradient of the field can be expressed as

$$|\vec{\nabla} E_{av}| = \frac{E_{max} - E_{min}}{d - R} \tag{7}$$

After normalization, so as to keep the breakdown voltage constant, Eq. (7) becomes

$$|\vec{\nabla} E_{av}| = E_{max} - E_{min} \tag{8}$$

Substituting the actual values of the maximum and minimum fields, we have

$$|\vec{\nabla} E_{av}| = \frac{V_T}{\cosh^{-1}\left(\frac{d}{R}\right)} \left[\frac{C}{2R(d-R)} - \frac{1}{C}\right] \tag{9}$$

or in simplified form

$$|\vec{\nabla} E_{av}| = \frac{V_T}{2R \cosh^{-1}\left(\frac{d}{R}\right)} \left(\frac{d/R - 1}{d/R + 1}\right)^{1/2} \tag{10}$$

Thus ∇E_{av} is seen to be a function of two geometric parameters: d/R and R. For $d/R \gg 1$, Eq. (10) reduces to

$$|\vec{\nabla} E_{av}| = \frac{V_T}{2R \ln \frac{2d}{R}} \tag{11}$$

In Fig. 3, ∇E_{av} is plotted against d/R in a semilog scale for different values of R. It is seen that the dependence is linear up to $d/R \sim 5$ and exponential beyond that. Moreover, the influence of R is seen to be crucial; the thinner the wire, the better.

Now, taking into consideration that the dielectrophoretic force is given as

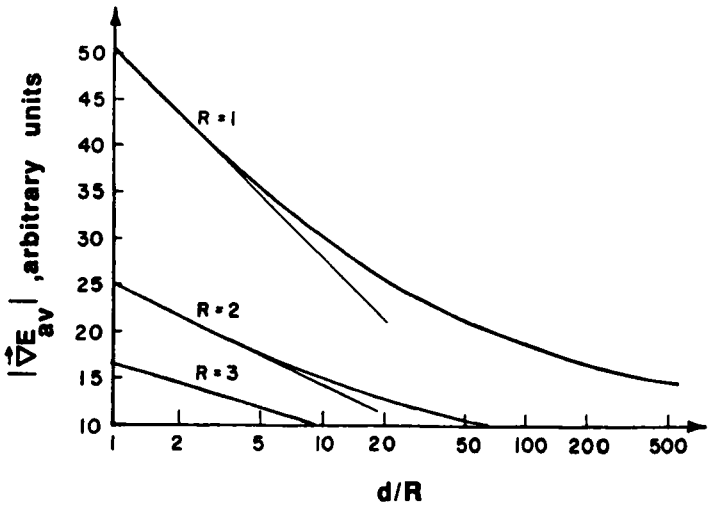

FIG. 3. Average gradient (arbitrary scale) between two wires for different values of d/R and R.

$$\vec{F}_d = \tfrac{1}{2}\alpha v \vec{\nabla} E^2 \tag{12}$$

where α is the polarizability and v is the particle volume, we should calculate ∇E_X^2 throughout the range $X = 0$ to $X = d - R$ to obtain a more accurate picture. Thus using Eq. (3) we have

$$|\vec{\nabla} E_X^2| = 4\left(\frac{V_T C}{\cosh^{-1}\left(\frac{d}{R}\right)}\right)^2 \frac{X}{(X^2 - C^2)^3} \tag{13}$$

∇E_X^2 is then plotted in Fig. 4 against a normalized abscissa.

It can be seen that for small d/R there is hardly a zone where the force tends to zero, while for large d/R the force exists only in the close vicinity of the wires, i.e., this is the situation where the wires do not interact, similar to the case of a single wire in a uniform applied field (*3*).

To quantify this finding, Fig. 5 shows the dependence of the gradient at the wire surface upon d/R, demonstrating clearly that the two cases referred to above are quite distinct. Both of them show a linear dependence in a log-log scale with an intermediate range at $2 < d/R < 20$.

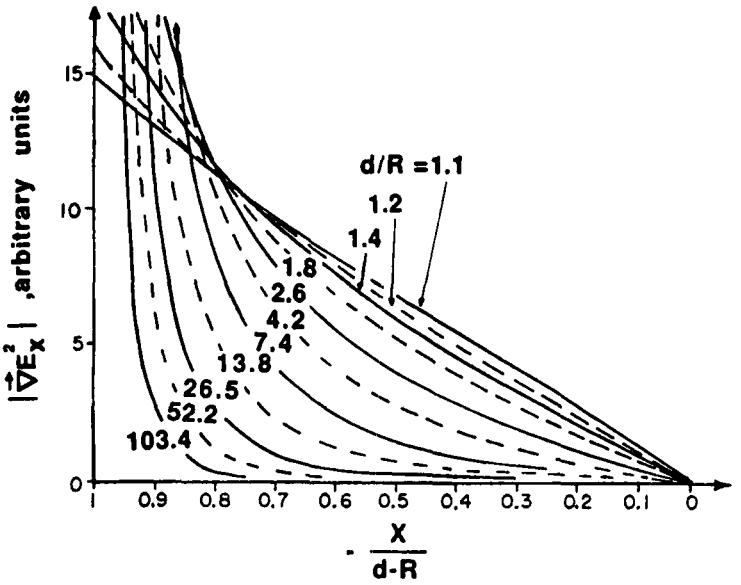

FIG. 4. Dielectrophoretic force as function of normalized distance for different values of d/R.

Extrapolated, the two straight lines intersect at $d/R \approx 5.5$; thus, it can be established that the best filtration yields should be obtained at $d/R < 5$.

III. MODELIZATION OF A LOADED FILTER

Because industrial filters are to be designed for prolonged stints of operation between flushings, it is important to know the particle buildup characteristics. This buildup is often called "load" and generally reaches a saturation value after a sufficiently long time. Flushing must be performed well before that time is reached because the filter is not effective close to saturation.

Thus, particulates removed from the liquid will form a time-dependent buildup on the wires, which is equivalent to a coating with its attendant variation both of the electric current passing through the liquid and of the actual field existing in the liquid under a constant applied voltage on the electrodes. A simple model for this scheme is shown in Fig. 6, where d, E, and σ denote thickness, field, and specific conductivity, respectively, while subscripts 1 and 2 refer to the coating and liquid. This plate-

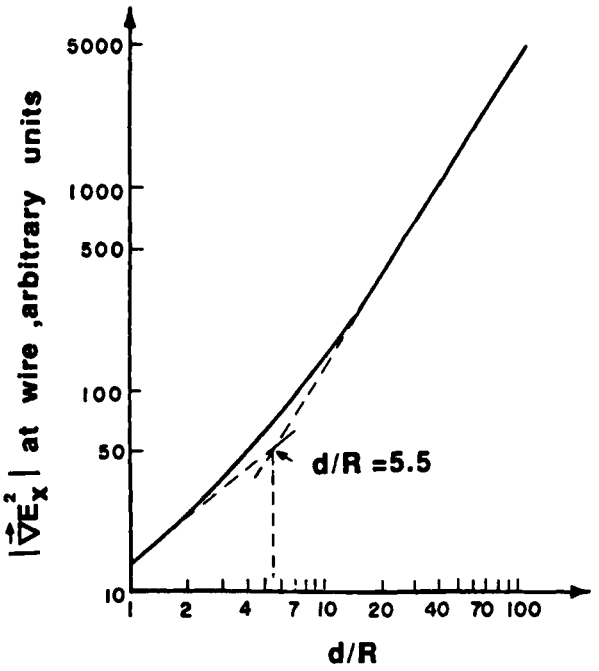

FIG. 5. Illustration of the two regimes for the force dependence on d/R.

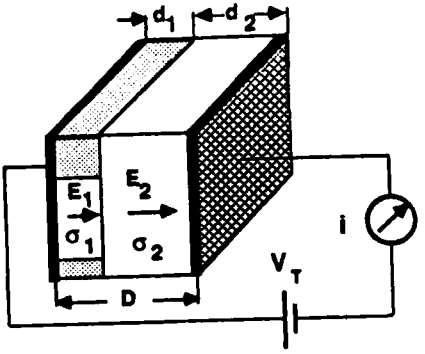

FIG. 6. Plate condenser model for the analysis of loading.

condenser analogy enables us to determine the insulation effect of the buildup accumulating in a comb pattern system of grids as shown in Fig. 1. Using the interfacial-polarization approach according to Maxwell (e.g., Ref. 5), we have the following.

At time $t = 0$, the electrical inductions D_1 and D_2 are equal since there are no charges trapped at the interface:

$$\varepsilon_1 E_1 = \varepsilon_2 E_2 \tag{14}$$

Taking into account that the conduction currents (per unit area) i_{c1} and i_{c2} differ in the two layers, an interfacial charge $Q_{1,2}$ appears. At time $t = \infty$, when equilibrium is established, $i_{c1} = i_{c2}$, but then

$$E_1 \sigma_1 = E_2 \sigma_2 \tag{15}$$

In the transient interval:

$$D_2 - D_1 = Q_{1,2} \tag{16}$$

$$\frac{dD_2}{dt} - \frac{dD_1}{dt} = \frac{dQ_{1,2}}{dt} \tag{17}$$

Thus, using the definition of the conduction current, we have

$$\frac{dQ_{1,2}}{dt} = i_{c1} - i_{c2} \tag{18}$$

Combining Eqs. (17) and (18), we obtain the differential equation

$$\frac{dD_2}{dt} - \frac{dD_1}{dt} = i_{c1} - i_{c2} \tag{19}$$

To describe the system fully, an additional relation is required:

$$d_1 E_1 + d_2 E_2 = V_T \tag{20}$$

Thus, two extreme situations exist, one at $t = 0$, for which

$$E_1 = \frac{V_T \varepsilon_2}{\varepsilon_1 d_2 + \varepsilon_2 d_1} \tag{21-1}$$

$$E_2 = \frac{V_T \varepsilon_1}{\varepsilon_1 d_2 + \varepsilon_2 d_1} \tag{21-2}$$

and the other at $t = \infty$, for which

$$E_1 = \frac{V_T \sigma_2}{\sigma_1 d_2 + \sigma_2 d_1} \tag{22-1}$$

$$E_2 = \frac{V_T \sigma_1}{\sigma_1 d_2 + \sigma_2 d_1} \tag{22-2}$$

Equation (21) represents the dielectric regime (permittivities only relevant) and Eq. (22) the conductive regime (conductivities only relevant). For $0 < t < \infty$ there is a transient regime described by two differential equations obtained by combining Eqs. (17) and (20). The one referring to E_2 reads:

$$\varepsilon_0 \frac{dE_2}{dt}(\varepsilon_2 d_1 + \varepsilon_1 d_2) + E_2(\sigma_1 d_2 + \sigma_2 d_1) = \sigma_1 V_T \tag{23}$$

Solving subject to the initial condition of Eq. (21-2), we obtain

$$E_2 = \frac{\sigma_1 V_T}{\sigma_1 d_2 + \sigma_2 d_1} + V_T\left(\frac{\varepsilon_1}{\varepsilon_1 d_2 + \varepsilon_2 d_1} - \frac{\sigma_1}{\sigma_1 d_2 + \sigma_2 d_1}\right)^{e^{-t/\tau}} \tag{24}$$

with

$$\tau = \varepsilon_0 \frac{\varepsilon_2 d_1 + \varepsilon_1 d_2}{\sigma_1 d_2 + \sigma_2 d_1}$$

The current i_2 can then be determined by using the relation

$$i_2 = i_{c2} + \frac{dD_2}{dt} \tag{25}$$

Combining Eqs. (24) and (25), we obtain

$$i_2 = \frac{V_T}{\sigma_1 d_2 + \sigma_2 d_1}\left[\sigma_1 \sigma_2 + d_1 d_2\left(\frac{\sigma_2 \varepsilon_1 - \sigma_1 \varepsilon_2}{\varepsilon_1 d_2 + \varepsilon_2 d_1}\right)^2 e^{-t/\tau}\right] \tag{26}$$

This derivation assumes constant d_1 and d_2, but in reality they are time-

dependent. The rate of increase of d_1 is not known *a priori* since it is governed by operational and geometrical factors, but we can take as a guide the model described by Guo et al. (*6*) on trapping of particulates in a magnetic field. As expected, an exponential relationship exists between d_1 and t:

$$d_1 = d_{1\max}(1 - e^{-\Lambda t}) \tag{27}$$

where

$$d_{1\max} = K(V_d/V_0)^{1/3} \qquad \text{and} \qquad \Lambda = f(c,V_0,a,b)$$

K is a constant, probably dependent on the Reynolds number of the particles (*15*), V_d is the dielectrophoretic velocity, and V_0 is the superficial flow velocity as described elsewhere (e.g., Ref. *18*):

$$\frac{V_d}{V_0} = \frac{4b^2E_0\varepsilon_0\varepsilon_f\gamma\beta}{3\eta a V_0} \tag{28}$$

a and b are, respectively, the wire and particle radii, E_0 is the initially applied field, ε_0 is the absolute dielectric permittivity for free space, ε_f is the relative dielectric permittivity of the fluid, γ and β are the rod and particle polarization factors, respectively, and η is the fluid viscosity.

Λ in Eq. (27) is a quantity characterizing the rate of growth of the layer. As only scanty information can be found in the literature, it can be assumed to be a function of the main geometric and operational parameters such as the particle concentration in the fluid c, V_0, a, and b.

To compute the current as a function of the time-dependent d_1, Eqs. (23) and (27) must be combined, yielding the following differential equation:

$$\frac{dE_2}{dt} = \frac{\sigma_1 V_T - E_2(a_1 + b_1 e^{-\Lambda t})}{\varepsilon_0(a_2 + b_2 e^{-\Lambda t})} \tag{29}$$

with the initial conditions $t = 0$ and $E_2 = V_T/D$, and the constants defined as

$$a_1 = \sigma_1 D + d_{1\max}(\sigma_2 - \sigma_1)$$
$$a_2 = \varepsilon_1 D + d_{1\max}(\varepsilon_2 - \varepsilon_1)$$
$$b_1 = d_{1\max}(\sigma_1 - \sigma_2)$$
$$b_2 = d_{1\max}(\varepsilon_2 - \varepsilon_1)$$

This equation is too complex for an analytical solution, so numerical data were obtained with a Runge-Kutta procedure. The values of some constants were kept unchanged for all calculations:

$$D = 0.01 \text{ m}$$

$$d_{1\max} = 0.005 \text{ m}$$

$$\varepsilon_1 = 4$$

$$\varepsilon_2 = 2$$

$$V_T = 1000 \text{ V}$$

In Fig. 7 the current variation is shown for three values of Λ (characterizing the rate of buildup of d_1) and for the three possibilities concerning the conductivities $\sigma_1 < \sigma_2$, $\sigma_1 = \sigma_2$, and $\sigma_1 > \sigma_2$ (Curves 1, 2, 3). For Case 1, as expected, the current is high at initial values of t and decreases as the insulating effect of d_1 becomes felt; for Case 2, no variation in the current is seen, since the conductivities are equal; Case 3 is the inverse of Case 1, i.e., increase of the current as d_1 gets thicker, with the additional feature that at large values of Λ (100 and 1000) the displacement current becomes very strong, causing a very significant transient effect.

Another interesting feature is exhibited by the behavior of d_1 in Fig. 8, compared with i in Fig. 7. It is seen that for $d_1 \approx d_{1\max}$, the current is the same in Cases 1 and 3; this, however, is expected since $d_{1\max}$ was chosen equal to $D/2$, so the situation is symmetric.

Figure 9 shows that on increasing the conductivity differential between the two layers the current maximum is shifted to the left while increasing at the same time—which leads to a situation where the curve becomes quite similar to the inverse case, i.e., $\sigma_1 < \sigma_2$.

The above model does not, however, always describe what is really happening. This is due to the earlier noted preferability of fields just below the breakdown voltage. Under these conditions the apparent conductivity of the liquid becomes nonlinear; in fact, the current is then given by (*16*):

$$i = \sigma_2 E^f \tag{30}$$

where f is a constant (>1) depending on the type of liquid. Thus, when a liquid containing suspended particles at low volume concentration is subjected to the action of a plate condenser as in Fig. 10(a), a field-line

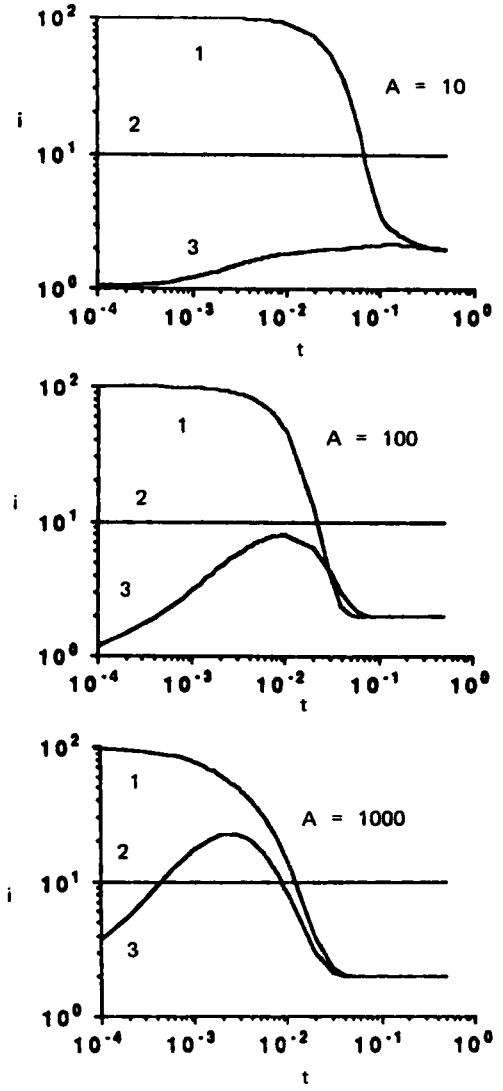

FIG. 7. Current dependence upon time for three values of Λ [t in s, i in $(A/m^2) \times 10^{-5}$]:

	σ_1	σ_2
(1)	10^{-10}	10^{-8}
(2)	10^{-9}	10^{-9}
(3)	10^{-8}	10^{-10}

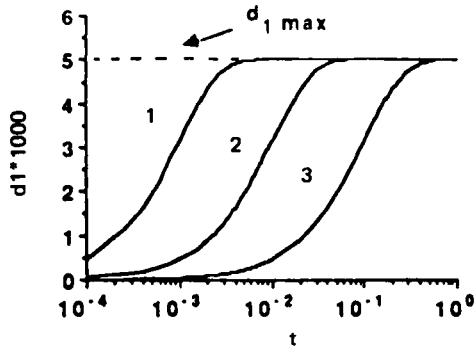

FIG. 8. Growth of layer d_1 for three values of Λ: (1) $\Lambda = 1000\ s^{-1}$, (2) $\Lambda = 100\ s^{-1}$, (3) $\Lambda = 10\ s^{-1}$.

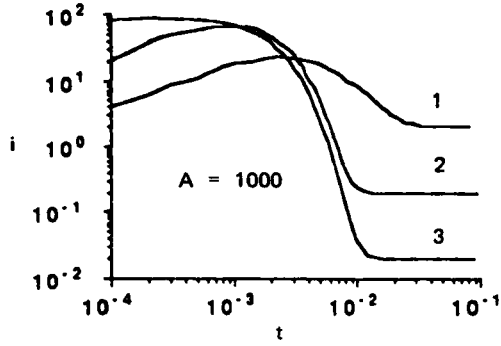

FIG. 9. Current dependence upon time for $\Lambda = 1000$ and $\sigma_1 > \sigma_2$ for various values of the conductivities:

	σ_1	σ_2
(1)	10^{-8}	10^{-10}
(2)	10^{-7}	10^{-11}
(3)	10^{-6}	10^{-12}

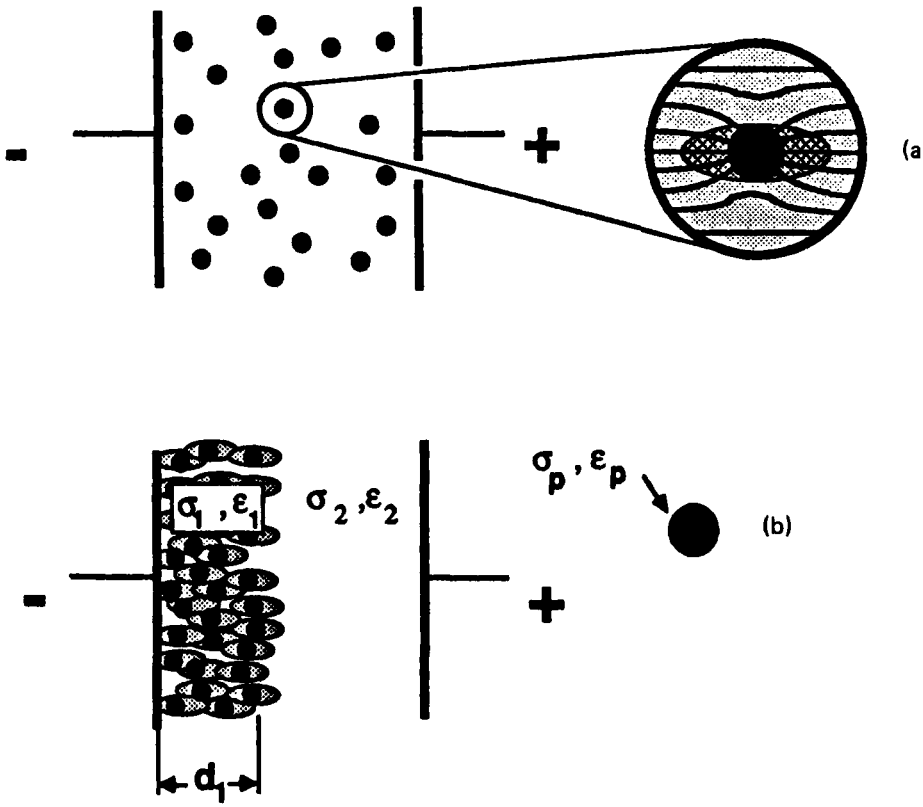

FIG. 10. Scheme explaining the influence of insulating particles on the increase of the conductivity current passing through a plate condenser. (a) Dilute suspension with close up of a particle showing the field line concentration around it. (b) Loosely packed layer featuring overlapping of high field regions, implying a percolation effect.

concentration forms around each particle—implying, in fact, the existence of a zone of higher conductivity (cross-hatched ellipse in close-up). Now, if the particles are part of a loosely packed layer as in Fig. 10(b), these zones may touch or overlap, causing percolation which is equivalent to having $\sigma_1 > \sigma_2$ in spite of the fact that $\sigma_p \ll \sigma_2$. Thus the combination of particles of permittivity $\varepsilon_p > \varepsilon_2$ with a liquid of higher conductivity makes for an increase of the current instead of a reduction as an insulating layer would be expected to act through the screen effect. This phenomenon was first discovered by Pohl and was also noticed by the authors in laboratory experiments which will be reported on a later occasion.

IV. PRACTICAL DESIGN

Design practice involves conflicting considerations: a solution may seem optimum from the physical viewpoint but unsound technologically or too expensive to realize and/or operate. Accordingly, one has to strive for a system as close as possible to the theoretical optimum but technologically simple and inexpensive. As noted in the Introduction, the conventional technique is based on concentric electrodes filled with beads. Use of grid electrodes entails far greater sophistication, with the following features:

Fine wire for very high gradients (<1 mm diameter).

Close spacing of the grids to ensure $d/R < 5$. Because fine wire grids lack rigidity, the system has to be stiffened by suitable spacers made of insulating and heat-resistant material (e.g., Teflon, pertinax).

Trapping in the flow direction so as to minimize the pressure drop across the filter and at the same time reduce the possibility of reentrainment.

Easy cleanability. Grids are obviously easier to clean than beads, because the open matrix lends itself to vibration under mechanical excitation and to flushing with air/oil mixtures at high flow velocities. The effectiveness of the cleaning process is indicated by restoration of the initial current reading.

In any kind of matrix, the following characteristics are mandatory:

Sufficient length to ensure high probability of particle trapping (>50 cm).

Sufficient cross section to ensure a low enough (<1 cm/s) flow velocity for retention of colloidal particles.

Provision for heating, with a view to reducing oil viscosity (when necessary) to a reasonable level (<10 cP) so as to minimize the drag effect.

In the light of the above, exact performance characteristics, especially those regarding the feed/flush cycle length, cannot be predicted without prior testing of the solid/liquid or liquid/liquid mixture at the laboratory and pilot levels. At best, mathematical models yield an approximate picture.

NOMENCLATURE

a	wire radius in Eq. (28)
a_1, a_2	constants in Eq. (29)
b	particle radius
b_1, b_2	constants in Eq. (29)
C	$(d^2 - R^2)^{1/2}$ (m)
c	impurities concentration (kg/m^3)
D	plate condenser width (m)
d	spacing of wires (m)
d_1, d_2	thickness of Layers 1 and 2 (m)
$d_{1\max}$	saturation value for Layer 1 (m)
E, E_0	electric field (V/m)
E_1, E_2	electric field in Layers 1 and 2 (V/m)
f	constant in Eq. (30)
K	constant in Eq. (27)
R	wire radius in Eq. (1) (m)
t	time (s)
V_0	superficial flow velocity (m/s)
V_b	breakdown voltage (V)
V_d	dielectrophoretic velocity (m/s)
V_T	applied voltage on electrodes in Eq. (29) (V)
v	particle volume (m^3)
X, Y	Cartesian coordinates

Greek

α	particle polarization (F/m)
β, γ	particle and wire polarizability factors
ε_0	absolute permittivity of vacuum (8.854×10^{-12} F/m)
$\varepsilon_1, \varepsilon_2$	relative permittivities of Layers 1 and 2
ε_p	relative permittivity of particles
η	dynamic viscosity (kg(m $\cdot$ s)$^{-1}$)
Λ	rate of growth for Layer 1 (s^{-1})
σ_1, σ_2	specific conductivity for Layers 1 and 2 ($\Omega \cdot$ m)$^{-1}$
σ	specific conductivity for particles ($\Omega \cdot$ m)$^{-1}$
τ	relaxation time in Eq. (24) (s)
ϕ	field potential (V)

REFERENCES

1. W. B. Boast, *Vector Fields,* Harper & Row, New York, 1964, p. 135.
2. C. S. Chen and H. A. Pohl, *Ann. N. Y. Acad. Sci., 238,* 176 (1974).
3. E. Durand, *Electrostatique et Magnétostatique,* Masson, Paris, 1953.
4. G. R. Fritsche, *Oil Gas J., 75*(13), 73 (1977).
5. R. Fournié, *Les isolants en électrotechnique, Concepts et théories,* Eyrolles, Paris, 1986.
6. B. J. Guo, T. J. Sheerer, M. Takayasu, and F. J. Friedlaender, *IEEE Trans. Magn., MAG-19*(1), 32 (1983).
7. F. J. Iglesias, M. O. Lopez, C. Santamaria, and A. Dominguez, *Biophys. J., 48,* 721 (1985).
8. T. B. Jones and G. M. Bliss, *J. Appl. Phys., 48,* 1412 (1977).
9. C. Jordan and G. Sullivan, *Fundamentals of Continuous Dielectric Separation of Minerals,* Presented at SME-AIME Fall Meeting, Albuquerque, New Mexico, 1985, Preprint 85-383.
10. L. A. Kaye and R. J. Fiocco, *Sep. Sci. Technol., 19*(11&12), 783 (1985).
11. I. J. Lin and L. Benguigui, *J. Electrost., 13,* 257 (1982).
12. I. J. Lin and T. B. Jones, *Ibid., 15,* 83 (1984).
13. L. Martin, P. Vignet, C. Fombarlet, and F. Lancelot, *Sep. Sci. Technol., 18*(14&15), 1455 (1983).
14. A. D. Moore, *Electrostatics and Its Applications,* Wiley, New York, 1973.
15. J. E. Nesset and J. A. Finch, "A Loading Equation for High Gradient Magnetic Separators and Application in Identifying the Fine Size Limit of Recovery," in *Proc. Int. Symp. Fine Particles Processing,* Las Vegas, Nevada, 1980, p. 1217.
16. H. A. Pohl, *Dielectrophoresis,* Cambridge University Press, New York, 1978.
17. S. Ramo, J. R. Whinnery, and T. Van Duzer, *Fields and Waves in Communication Electronics,* Wiley, New York, 1965, p. 186.
18. A. L. Shalom and I. J. Lin, *J. Electrost., 18,* 39 (1986).
19. A. L. Shalom and I. J. Lin, *Sep. Purif. Methods, 16*(1), 1 (1987).
20. W. Walkenhorst, *Aerosol Sci., 1,* 225 (1970).
21. L. C. Waterman, *Chem. Eng. Prog., 61*(10), 51 (1965).
22. R. M. Wham and C. H. Byers, *Sep. Sci. Technol., 22*(2&3), 447 (1987).
23. T. J. Williams and A. G. Bailey, *IEEE Trans. Ind. Appl, IA-22*(3), 536 (1986).
24. G. Zebel, *J. Colloid Sci., 20*(6), 522 (1965).

Received by editor September 9, 1987
Revised February 25, 1988